Eur. Phys. J. A **17**, 439–443 (2003)
DOI 10.1140/epja/i2002-10189-2

THE EUROPEAN PHYSICAL JOURNAL A

Spectral function at high E_m and P_m

D. Rohe[a]

For the E97-006 Collaboration
Department of Physics and Astronomy, University of Basel, CH-4056, Basel, Switzerland

Received: 1 November 2002 /
Published online: 15 July 2003 –

Abstract. Experiment E97-006 was performed at JLab in Hall C to measure the spectral function $S(E_m, P_m)$ via (e, e′p) for the nuclei C, Al, Fe, Au in the region of high missing energy E_m and missing momentum P_m. To study short-range correlations as well as the reaction mechanism beyond PWIA data were taken in parallel and perpendicular kinematics covering a P_m range of up to 800 MeV/c. Assuming PWIA the spectral function can be extracted from the data. Preliminary results of the spectral function are compared to the Correlated Basis Function theory of Benhar and the Green's function approach of Müther *et al.*. The spectral functions obtained for different targets are compared as well.

PACS. 21.10.-k Properties of nuclei; nuclear energy levels – 25.30.-c Lepton-induced reactions

1 Introduction

The spectral function $S(E, k)$ describes the probability to find a proton with energy E and initial momentum k in the nucleus. Experimentally it can be accessed via (e, e′p) scattering on nuclei, *e.g.*, ^{12}C(e, e′p)^{11}B. In the Plane-Wave Impulse Approximation (PWIA) the virtual photon knocks out one of the protons of carbon, which, according to the shell model, are located in the single-particle shells $1s_{1/2}$ and $1p_{3/2}$. The residual nucleus ^{11}B can be left in an excited state. The initial energy E of the proton is defined as the difference between the energies of the initial and final nucleus, which is equal to the binding energy of the shell ϵ_B (≤ 0) plus ϵ_F (≤ 0) minus the excitation energy ϵ of the residual nucleus. The energy ϵ_F corresponds to the separation energy. Experimentally one cannot measure the excitation energy of the residual nucleus directly, but reconstruct the so-called missing energy E_m. The missing energy equals the difference of the initial and final energy of the electron minus the kinetic energies of the knocked-out proton and the residual nucleus. Further, one obtains the missing momentum P_m as the difference of the momentum transfer q and the final proton momentum. In PWIA one identifies the missing energy E_m with the absolute value of the initial energy E and the missing momentum P_m with the initial momentum $-k$ of the proton inside the nucleus.

The simplest theoretical description of the momentum distribution is provided by the Independent Particle Shell Model (IPSM). It makes the assumption, that the nucleons move independently in an averaged potential. This potential is obtained either by a Hartree-Fock calculation using an empirical effective nucleon-nucleon interaction, or taken as an optical potential usually in a Wood-Saxon shape, the parameters of which are fixed by elastic proton scattering on the specific nucleus. The energy distribution of the nucleons in the nucleus is typically described by a sum of Lorentzians centered at the energy eigenvalue of the various shells. The width Γ accounts for the experimentally determined energy broadening of the shell, which is related to the lifetime τ of the single-particle state by $\Gamma = 1/\tau$. This simple model explains the magic numbers of closed shells of nuclei as well as the charge and matter distribution of the nucleus. Further, it reproduces the shape of the momentum distributions reasonably well, provided the calculated distributions are multiplied with a factor less than one. This factor is called spectroscopic factor Z_α and can be obtained by integrating the experimental momentum distribution of a shell α over its missing-momentum distribution.

The spectroscopic factor Z_α gives the number of nucleons which reside in the shell α. Experimentally, one observes a depletion of the occupation number in the shell of about 30%. Depletion occurs also in other systems such as atoms, where it amounts only to about 0.2% for, *e.g.*, Ar, whereas in liquid ^{3}He the depletion reaches 50–60%. This indicates that the depletion increases with increasing strength of the interaction between the particles in the system. Indeed, the observed depletion lies in the repulsive core of the nucleon-nucleon interaction, which leads to scattering between particles at short distances. These Short-Range and tensor Correlations (SRC) lead to large missing energies and momenta. If the proton, which is

[a] e-mail: daniela.rohe@unibas.ch

strongly correlated with another proton is knocked out, the second proton leaves the nucleus with the opposite initial momentum due to momentum conservation. In this simple picture the missing energy would be equal to $E_{\rm m}= {P_{\rm m}}^2/(2M)$. Therefore, the maximum of the spectral function in the region of large $E_{\rm m}$ and $P_{\rm m}$ is expected at this position.

One of the consequences of SRC is the depletion of the single-particle region, since a fraction of the protons has energies and momenta far above the ones calculated in the IPSM. The experiment E97-006 took data in this region of large $E_{\rm m}$ and $P_{\rm m}$.

2 Recent theoretical calculations

The spectral function for ^{12}C extracted from the data will be compared to two recent theories, the Correlated Basis Function (CBF) theory of Benhar *et al.* [1] and the Green's function approach of Müther *et al.* [2].

In the CBF theory the spectral function is separated into two parts, the single-particle and the correlated spectral function. The single-particle spectral function dominates at small initial momentum k and energy E and describes mainly the shell structure of the specified nucleus. This part is taken from the IPSM model with a normalization of 0.78 given by the strength of the correlated part calculated in the CBF theory. The latter one is dominant at large initial momentum and is calculated from basis states which already take SRC and tensor correlation into account. The correlated spectral function is calculated for different densities of nuclear matter first. The strength at large k increases with incresing nuclear density. The spectral function for finite nuclei is obtained by using the Local Density Approximation (LDA).

The Green's function approach starts from a nucleon-nucleon interaction, which leads via the Bethe-Goldstone equation to the G-matrix of nuclear matter. From this the self-energy Σ can be derived. The hole states are represented by oscillator functions and the particle states by plane waves. In addition to the Hartree-Fock term the $2p1h$ and the $2h1p$ contributions are taken into account as corrections $\Delta\Sigma$ to the self-energy. The Green's function is obtained by inserting $\Delta\Sigma$ into the Dyson equation, which is solved in a momentum limited spherical model space. This leads to two solutions. For small momenta ($\leq k_{\rm F}$) the single-particle states are described including SRC, Long-Range Correlations (LRC) as well as the shell structure. The continuum part at large momenta ($k > k_{\rm F}$) is mainly caused by SRC. The spectral function is obtained by the imaginary part of the Green's function.

3 Setup and kinematics of the experiment

The experiment was performed in Hall C at JLab. The incident electron energy was 3.2 GeV. The scattered electrons were detected in the HMS spectrometer and the knocked-out protons in the SOS spectrometer. Both spectrometers are equipped with two drift chambers as well as four scintillator planes and a Čerenkov detector.

Data for H_2 and ^{12}C on top of the quasi-elastic peak were taken for calibration and check. Angle and momentum offsets were determined for both spectrometers from the redundance in the hydrogen kinematics. The transmission of the proton from the target through the different materials in the spectrometer was determined $(95.5\pm1)\%$, which is in agreement with the value obtained from the interaction length of the various materials. The cross-section of the reaction H(e, e′p) in the range of 0.6 to 2.3 $(\mathrm{GeV}/c)^2$ is in good agreement with previous data and the fit of Mergell *et al.* [3]. The statistical error is negligible, the systematic uncertainty amounts to 3.5% due to the uncertainty in beam energy ($\pm5\cdot10^{-4}$), in the electron angle (±1 mrad) as well as uncertainties in current measurement, detector efficiencies, etc.

The data taken for ^{12}C(e, e′p) in the single-particle region were compared to the prediction using the IPSM model. The shell structure of ^{12}C, clearly visible in the missing-energy distribution, is well reproduced by the IPSM model. To compare the yield of the data to the IPSM prediction cuts in $E_{\rm m}$ ($\leq$ 50 MeV) and $P_{\rm m}$ (≤ 200 MeV/c) were applied. This leads to a ratio of data to IPSM yield of 0.84 at $Q^2 = 1.9$ $(\mathrm{GeV}/c)^2$ using a transparency factor for carbon T(C) of 0.6. This result must not be compared with the spectroscopic factor of 0.65, because the cuts used for this analysis already include part of the strength due to the contribution of SRC. The applied cuts correspond to the ones usually used in transparency measurements. A recent measurement of the transparency factor of Garrow *et al.* [4] leads to $T(\mathrm{C}) \approx 0.55$ using a spectroscopic factor of 0.9 in agreement with previous transparency measurements.

Production data were taken for C, Al, Fe, and Au covering a wide range of $E_{\rm m}$ and $P_{\rm m}$ (up to 800 MeV/c). For each target three settings were measured in parallel kinematics and two in perpendicular kinematics. The purpose of performing the experiment in perpendicular as well as in parallel kinematics is to study contributions to the reaction mechanism beyond PWIA. Rescattering can occur after the (e, e′p) process due to an additional proton-nucleon scattering inside the nucleus. This leads to the wrong values for the reconstructed $E_{\rm m}$ and $P_{\rm m}$.

Another process is the excitation and the decay of the Δ-resonance, which leads to an additional undetected pion. Due to the mass and the energy of the pion, the reconstructed $E_{\rm m}$ is larger than the initial one. This process can only occur for $E_{\rm m} > 150$ MeV. In parallel kinematics it is expected that rescattering is suppressed because of the smaller phase space. Further, the influence of the Δ-resonance should be less than in perpendicular kinematics because of its transversal character.

4 Extraction of the spectral function

Despite these complications, for the time being we assume PWIA to extract the spectral function from the data and

treat the mentioned processes as corrections at a later time. Then, the experimental cross-section is proportional to the e-p off-shell cross-section, the spectral function and the nuclear transparency T. As e-p off-shell cross-section the cc1 version of de Forest is used [5]. The nuclear transparency factor accounts for the absorption of the proton inside the nucleus. These factors were measured in various experiments (*e.g.*, [4]), but will lead to a systematic error of $\approx 10\%$. The values used in the analysis are 0.6, 0.5, 0.4, 0.3 for C, Al, Fe and Au, respectively. The data are binned in E_m and P_m. The bin size of E_m varies between 10 and 50 MeV depending on the statistics, whereas the bin size for P_m is fixed at 40 MeV/c. Background subtraction is performed using the coincidence time spectrum (FWHM = 0.5 ns), which was corrected for start time differences of the trigger signal generated by various scintillator paddles as well as path length differences of the particles in the spectrometers. The events in each (E_m, P_m) bin are corrected for the efficiency of the detectors and the tracking algorithms. The beam current was measured by beam cavity monitors tuned to match the beam bunch frequency. These monitors were frequently calibrated against the UNSER monitor, which is based on magnetic induction by the electron beam. The phase space was taken from the Hall C Monte Carlo simulation. The so-obtained spectral function has to be corrected for radiative processes, which shifts events from one (E_m, P_m) bin to another. For the radiative processes the formalism of [6] is used, which accounts both for radiative corrections of electron and the proton. The spectral function is corrected by multiplying the ratio of events obtained in a Monte Carlo simulation[1] without and with radiative processes. For this a spectral function is needed. It is taken from a fit to the spectral function extracted from the data combined with the IPSM contribution for low E_m, P_m. Convergence between model and experimental spectral function is reached in an iterative process.

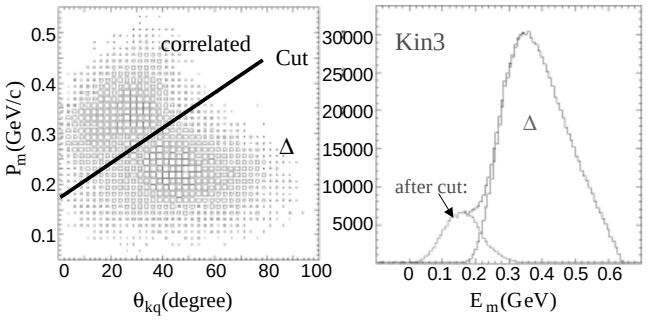

Fig. 1. Left: cut used to separate the Δ-resonance from the correlated region. Right: after applying this cut to the data the small bump representing the correlated region remains. Subtraction of the correlated region from the data leads to the region indicated by Δ.

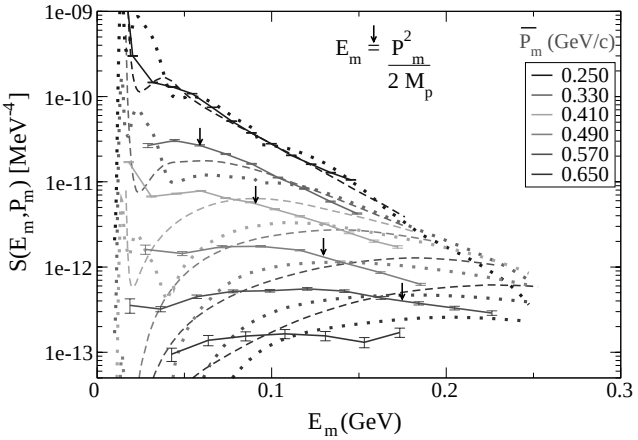

Fig. 2. Distorted spectral function in parallel kinematics (solid lines) compared to the theory of Benhar [1] (dashed lines) and to the Green's function approach of [2,4] (dotted lines) for selected missing momenta (see legend). The arrows indicate the position at which one would expect the maximum of the spectral function according to the simple picture described in the text.

5 Comparison to theories

The preliminary result for the spectral function in parallel kinematics will be compared to the CBF theory [1] and the Green's function approach [2] in the following. Because the theories do not describe the Δ-resonance, the correlated region in the experimental spectral function has to be separated from the Δ-region. To some extent this can be with a cut in the 2-dimensional plot of P_m and θ_{kq}, which is the angle between the initial momentum k and the momentum transfer q. As can be seen in the left panel of fig. 1 the correlated strength in the parallel kinematics occurs at smaller angles and larger P_m than the Δ-resonance. This procedure can only work for data measured in parallel kinematics, not for the perpendicular kinematics. To demonstrate its effect the histogram of the E_m distribution of Kin3 is shown without and with the cut applied. The curve for the Δ-resonance is obtained by subtracting the cut spectrum from the raw one. From a comparison of the curves one concludes that the correlated region seems to be well separated from the Δ-resonance. It should be mentioned that the chosen kinematics Kin3, which covers the highest P_m in parallel kinematics, contains the largest contribution of the Δ-resonance. For the P_m distribution similar results are obtained.

In fig. 2 a selection of various P_m-bins for the spectral function measured for carbon in parallel kinematics (solid lines) is shown together with the predictions from the CBF theory (dashed lines) and the Green's function approach (dotted lines). Both theories are in remarkable agreement at $P_m = 250$ MeV/c. With increasing P_m the agreement gets worse. The strength of both theoretical spectral functions is located at too large E_m. The maximum of the theoretical spectral functions is close to $E_m = {P_m}^2/(2M)$,

[1] Monte Carlo simulation of the Hall C Collaboration at Jefferson Lab.

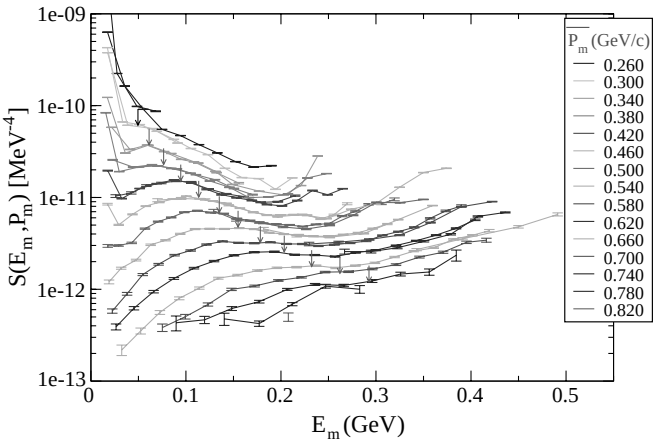

Fig. 3. Distorted spectral function extracted from the data in perpendicular kinematics for different P_{m}-bins.

where it is expected according to the simple picture of SRC mentioned above. This is not supported by the experimental result. The missing strength of the theories at low missing energy might indicate that LRC are much more important, even though LRC are included in the Green's function approach. In addition, the CBF theory is about a factor 2 larger than the experimental result in the high P_{m}-region. On the other hand, the integrated strength of the CBF prediction is in good agreement with the experiment (see sect. 7).

6 Results in perpendicular kinematics

The results for the spectral function extracted from the data in perpendicular kinematics are quite different from the one in parallel kinematics. The Δ-resonance cannot be separated as was done in the parallel kinematics. Therefore a cut was applied to select a region, where the contribution of the Δ-resonance is less important. The ratio of the data to the Monte Carlo simulation based on the spectral function from the CBF theory amounts to a factor of ≈ 3. This is probably due to rescattering processes, which are currently calculated by C. Barbieri. We also note that radiative corrections are much more important at large E_{m}. This can be clearly seen by comparing the results of a Monte Carlo simulation with and without inclusion of radiative processes.

The experimental spectral function in perpendicular kinematics is shown in fig. 3 for various P_{m}-bins. Surprisingly the maximum of the spectral function in the correlated region follows the position expected from the simple picture of SRC mentioned above. This position is indicated by the arrows. But this obviously cannot be taken as a signature of SRC, because the origin of much of the strength lies in rescattering processes and the contribution of the Δ-resonance.

7 Momentum distribution

To make a better comparison between the spectral functions obtained in parallel and perpendicular kinematics and the ones provided by theory, the momentum distribution is calculated:

$$n(P_{\mathrm{m}}) = \int_{\epsilon_{\mathrm{F}}}^{\infty} \mathrm{d}E_{\mathrm{m}} S(E_{\mathrm{m}}, P_{\mathrm{m}})\,. \tag{1}$$

Because we are interested in the correlated region, the lower limit is set to 40 MeV. This insures that most of the single-particle strength is excluded. The upper integration limit is chosen such that it excludes as well as possible the region of the Δ-resonance and depends on the P_{m}-bin. The comparison of the experimental $n_{\mathrm{exp}}(P_{\mathrm{m}})$ momentum distribution in parallel kinematics to the theoretical one from the CBF and Green's function approach ($n_{\mathrm{CBF}}(P_{\mathrm{m}})$ or $n_{\mathrm{GF}}(P_{\mathrm{m}})$, respectively) shows, that for $P_{\mathrm{m}} \leq 450$ MeV/c $n_{\mathrm{exp}}(P_{\mathrm{m}})$ agrees within $\pm$ 20% with $n_{\mathrm{CBF}}(P_{\mathrm{m}})$, but is a factor of 1.5 higher than $n_{\mathrm{GF}}(P_{\mathrm{m}})$. For $P_{\mathrm{m}} \geq 500$ MeV/c $n_{\mathrm{CBF}}(P_{\mathrm{m}})$ exceeds the experimental one by a factor of ≈ 2, whereas $n_{\mathrm{GF}}(P_{\mathrm{m}})$ is approaching $n_{\mathrm{exp}}(P_{\mathrm{m}})$ from above. The momentum distribution measured in perpendicular kinematics exceeds both theories by more than a factor of 2. One should keep in mind, that these results are dependent on the lower limit of the integral eq. (1). Similarly, one also can compare the missing energy averaged over each P_{m}-bin. The averaged missing energy $\overline{E_{\mathrm{m}}}$ is larger for both theories, which yield very similar results. The deviation to the experiment increases with increasing P_{m}. By integrating the momentum distribution over P_{m} in the range of 230 to 630 MeV/c one obtains the averaged number of protons Z_{C} detected in the correlated region (= "correlated strength"). Within 20% there is agreement between experiment and both theories in parallel kinematics, whereas in perpendicular kinematics the data are a factor of 3 too high.

8 Comparing the spectral function of different nuclei

So far only the results for the spectral function for carbon were discussed. In this section the spectral function extracted from the data for Al, Fe and Au in both parallel and perpendicular kinematics will be compared to the one of carbon. To make a reasonable comparison the spectral function of different nuclei is normalized to the number of protons in each nucleus. In fig. 4 the so-normalized spectral function in parallel kinematics is shown for selected P_{m}-bins. In the correlated region the spectral functions extracted for C, Al, Fe are in fair agreement, whereas for increasing E_{m} they start to deviate, especially in the dip region between the correlated region and the Δ-resonance. The gold data lead to a spectral function far above the ones corresponding to the lighter nuclei. To perform a

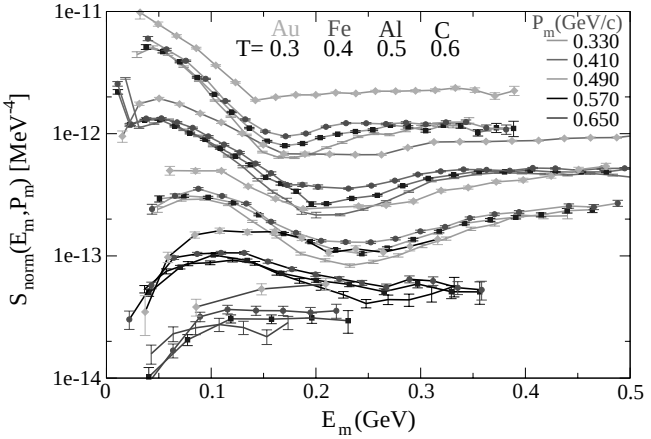

Fig. 4. Distorted spectral function for selected P_m-bins for Au (diamonds), Fe (circles), Al (squares) and C (no symbols) normalized to the number of protons in each nucleus. The transparency factors used in the analysis are also shown.

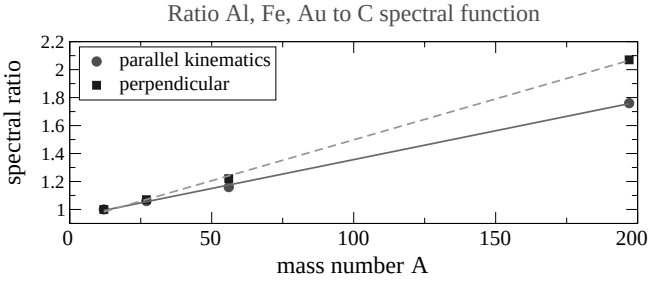

Fig. 5. Ratio of the spectral functions obtained for Al, Fe, and Au to the one using C are plotted against the mass number A.

more quantitative analysis the normalized spectral function of Al, Fe and Au is divided by the one of C. The result is averaged over the correlated region and plotted in fig. 5 against the mass number of C, Al, Fe and Au. These results do depend on the transparency factor used, which, however, is known to be better than 10%. Systematic errors will cancel to first order in the ratio of the spectral functions. The statistical uncertainty is small. The various uncertainties cannot explain the large enhancement of the spectral function of gold by a factor of 2 relative to the one of carbon. For Al (Fe) the enhancement is only 5% (20%). It is remarkable, that these values are nearly identical for parallel and perpendicular kinematics, except for the Au/C ratio.

It is likely that part of the enhancement of the spectral function for heavy nuclei is caused by the excess of neutrons in these nuclei. This leads to a larger number of n-p pairs involving a neutron and proton in a $^3S_1$ state, which results in additional SRC. Calculations of Ryckebusch [7] for ^{16}O(e, e′p) confirm that the contribution of tensor correlations exceeds the one from central correlations by up to a factor of 5.

9 Summary

The purpose of experiment E97-006 is to study SRC and the reaction mechanism beyond PWIA. For that, data were taken on different targets C, Al, Fe, Au in parallel as well as in perpendicular kinematics. Rescattering processes should be pronounced in the perpendicular kinematics. In addition the contribution of the Δ-resonance should be enhanced. The distorted spectral functions were extracted under the assumption of PWIA from all data sets. A large difference in shape and magnitude between the spectral functions from the data in parallel and perpendicular kinematics is observed. The preliminary results were compared to the Correlated Basis Function theory [1] and the Green's function approach [2]. So far, none of the theories can describe the data. The agreement with the spectral function extracted from the parallel kinematics is always better than a factor of 2, while the integrated strength in the correlated region is well predicted. Both theories have the strength of the spectral function shifted to larger E_m, with the maximum of the calculated spectral function approximately fulfilling the relation $E_m = P_m{}^2/(2M)$. In fact the spectral function from perpendicular kinematics roughly obeys this relation, but this cannot be taken as a signature of SRC. Rescattering processes and the Δ-excitation are largely responsible for this strength. The calculation of the rescattering processes by Barbieri should help to understand the different behavior of the distorted spectral function obtained in parallel and perpendicular kinematics.

The distorted spectral functions of Al, Fe, Au were compared to the one of C. The ratios of the spectral functions of heavier nuclei to the one of C were obtained and averaged over the correlated region. For this comparison the spectral functions were normalized to the number of protons in the nucleus. This ratio increases with the mass number and may largely result from the fact that for heavy $N \neq Z$ nucleus the short-range correlations mainly result from the interaction of n-p pairs, which increase with Z more rapidly than the number of protons.

References

1. O. Benhar, A. Fabrocini, S. Fantoni, I. Sick, Nucl. Phys. A **579**, 493 (1994).
2. H. Müther, G. Knehr, A. Polls, Phys. Rev. C **52**, 2955 (1995).
3. P. Mergell, U.-G. Meissner, D. Drechsel, Nucl. Phys. A **592**, 367 (1996).
4. K. Garrow *et al.*, Phys. Rev. C **66**, 044613 (2002), hep-ex/0109027.
5. T. de Forest, Nucl. Phys. A **392**, 232 (1983).
6. R. Ent, W. Filippone, C.R. Makins, R.G. Milner, T.G. O'Neill, T.A. Wasson, Phys. Rev. C **64**, 054610 (2001).
7. J. Ryckebusch, S. Janssen, W. Van Nespen, D. Debruyne, Phys. Rev. C **61**, 021603 (2000).